Spontaneous Polaron Transport in Biopolymers

B. Chakrabarti[1] [(a)], B. M. A. G. Piette[1] [(b)] and W. J. Zakrzewski[1] [(c)]

[1] *Department of Mathematical Sciences, Durham University, Durham, DH1 3LE, United Kingdom.*

PACS 71.38.-k – Polarons in electronic structure of solids
PACS 87.15.-v – Biomolecules: structure and physical properties
PACS 03.75.lm – solitons

Abstract –Polarons, introduced by Davydov to explain energy transport in α-helices, correspond to electrons localised on a few lattice sites because of their interaction with phonons. While the static polaron field configurations have been extensively studied, their displacement is more difficult to explain. In this paper we show that, when the next to nearest neighbour interactions are included, for physical values of the parameters, polarons can spontaneously move, at $T = 0$, on bent chains that exhibit a positive gradient in their curvature. At room temperature polarons perform a random walk but a curvature gradient can induce a non-zero average speed similar to the one observed at zero temperature. We also show that, at zero temperature, a polaron bounces on sharply kinked junctions. We interpret these results in light of the energy transport by transmembrane proteins.

Introduction. – Proteins, essential components of all biological cells are central to their proper functioning. As "form determines function", a study of protein structure and dynamics is of utmost importance in elucidating their role in cellular behaviour. One of the key problems in biology is to understand energy transport from one part of the cell to another and to study the role of protein conformations and conformational transitions in this process.

The mechanism of charge and energy transport in proteins and other bio-macromolecules at the atomic scale was proposed Davydov and co-workers [1]. In this approach the transport properties are considered in terms of the emergence of a 'polaron' whose properties and dynamics are used to describe the resultant transport. The polaron describes a localised excitation which carries energy corresponding to some vibrational modes of a group of molecules and a distortion of the chain containing these molecules. The system acts as a particle and its dynamical properties can be studied in terms of solutions of particular differential equations that describe its behaviour.

The Davydov theory hinges on the assumption that an extra electron or energy quanta released in the hydrolysis of ATP (adenosine triphosphate) can be stored by the protein molecule in its vibrational mode. The nonlinear coupling between the chain vibrational modes and the electron leads to the formation of a polaron which as it propagates along the polypeptide backbone leads to energy/charge transport. The soliton mediated transport mechanism has been applied to helical proteins [2] and is reviewed in [3,4]. Most polaron studies are based on simple one-dimensional model but recent studies also considered two and and three-dimensional models [5–8].

Studies of polaron transport on α helical polymers have recently been reported by Henning [9–12]. However, in most of these studies the polaron is "kicked" from its rest state via a perturbation [13]. In this paper we look at the spontaneous polaron transport via charge-conformational coupling. In particular, we study polaron transport on a flexible chain with an imposed initial bend at both zero ($T = 0$) and non-zero ($T \neq 0$) temperatures. We now summarise our main results.

At $T = 0$ a polaron can undergo spontaneous motion via the coupling of charge with the conformational degrees of freedom. Thus an imposed bend on the chain causes the polaron to accelerate. However, we have found that when such an accelerating polaron encounters a kink, a slope discontinuity along the chain backbone, it gets reflected instead of continuing along its original direction of motion guided by inertia. The reason for this due to the long-range nature of the exchange coupling term. At finite temperature $T \neq 0$ thermal fluctuations wash away directed

[(a)] E-mail: buddhapriya.chakrabarti@durham.ac.uk
[(b)] E-mail: b.m.a.g.piette@durham.ac.uk
[(c)] E-mail: w.j.zakrzewski@durham.ac.uk

transport and the polaron undergoes large amplitude fluctuations about its mean position. However, since the chain ends act as reflecting walls, a polaron formed closer to one end of a straight chain would often get reflected, resulting in an overall small but non-negligible drift.

The paper is organised as follows: In the next section we present the Hamiltonian describing polaron transport on a flexible chain and change variables to dimensionless quantities. The dimensionless parameter values corresponding to physically relevant systems *e.g.* proteins are computed in Sec.3. We describe the results of our numerical studies in Sec.4 and we set our work in perspective in the final section.

Polaron Hamiltonian on a Flexible Chain. – We consider a modified version of the polaron model proposed by Mingaleev *et al.* [14]. Our model involves a semi-classical treatment of the interaction between a phonon field $\vec{R}_n$ and an electron field ϕ_n on a flexible linear chain whose nodes are labelled by an index n.

The Hamiltonian of the model is given by

$$\begin{aligned} H &= \sum_n \left[\frac{\hat{M}}{2} \left(\frac{d\vec{R}_n}{d\tau} \right)^2 + \hat{U}_n(\vec{R}) - \frac{1}{2}\Delta|\phi_n|^4 \right. \\ &\left. + W \left(2|\phi_n|^2 - \sum_{m \neq n} J_{nm}\phi_n^*\phi_m \right) \right], \end{aligned} \quad (1)$$

where M is the mass of the chain node, W is the linear excitation transfer energy and Δ the non-linear self-trapping interaction. The excitation transfer coefficients $J_{n,m}$ are of the form:

$$J_{n,m} = J(|\vec{R}_n - \vec{R}_m|) = (e^{\alpha} - 1)\, e^{-\alpha|\vec{R}_n - \vec{R}_m|/a}, \quad (2)$$

where α^{-1} sets the relative length scale over which the interaction decreases, in units of a, and where a is the rest distance between two adjacent sites. The $J_{n,m}$ describes the long range interaction between the electron field at different lattice sites n and m; its value decreases exponentially with the distance between them.

Note that the normalisation of the electron field is preserved in our model, *i.e.*

$$\sum_n |\phi_n|^2 = 1. \quad (3)$$

The phonon potential U_n consists of three terms:

$$\begin{aligned} \hat{U}_n(\vec{R}) &= \frac{\hat{\delta}}{2} \sum_{m \neq n} (\hat{d} - |\vec{R}_n - \vec{R}_m|)^2 \Theta(\hat{d} - |\vec{R}_n - \vec{R}_m|). \\ &+ \frac{\hat{\sigma}}{2}(|\vec{R}_n - \vec{R}_{n-1}| - \hat{a})^2 + \frac{\hat{k}}{2} \frac{(\theta_n - \varphi_n)^2}{[1 - ((\theta_n - \varphi_n)/\theta_{max})^2]} \end{aligned} \quad (4)$$

The first term in Eq.(4) models the elastic energy describing the stretching of the adjacent nodes of the chain, where $\hat{a}$ is the equilibrium separation between them. The second term describes the bending energy of the chain akin to semi-flexible polymers. Here θ_n is the angle between $\vec{R}_n - \vec{R}_{n-1}$ and $\vec{R}_{n+1} - \vec{R}_n$, φ_n is the rest angle between these adjacent lattice links and θ_{max} is the largest angle allowed. In the Mingaleev model [14] $\varphi_n = 0$ and the equilibrium configuration of the chain is a straight one. Non-zero values of φ_n lead to a bent chain. The last term, (proportional to $\hat{\delta}$), models hard-core repulsion between the atoms of the chain. However, we note that this term does not contribute significantly in determining the equilibrium chain conformation.

In this paper symbols denoted by an overhead carat sign *e.g.* $\hat{M}$, $\hat{\sigma}$ *etc.* correspond to physical variables carrying units and dimensions while those without it correspond to non-dimensional variables and parameters. We rescale time τ by defining a timescale $\tau_0 = \frac{\hbar\Delta}{W^2}$s and rescale distances by a length scale a. The non-linear coupling parameter g appears as a dimensionless ratio of two energy scales.

$$\tau = t\tau_0 \qquad g = \frac{\Delta}{W} \qquad r = \frac{R}{a}. \quad (5)$$

In terms of these variables the Hamiltonian takes the form

$$\begin{aligned} H &= \frac{W^2}{\Delta} \sum_n \left[\frac{M}{2} \left(\frac{d\vec{r}_n}{dt} \right)^2 + U_n(\vec{r}) \right. \\ &\left. + g \left(2|\phi_n|^2 - \sum_{m \neq n} J_{nm}\phi_n^*\phi_m \right) - \frac{g^2}{2}|\phi_n|^4 \right], \end{aligned} \quad (6)$$

where

$$\begin{aligned} U_n(\vec{r}) &= \frac{\sigma}{2}(|\vec{r}_n - \vec{r}_{n-1}| - a)^2 + \frac{k}{2} \frac{(\theta_n - \varphi_n)^2}{[1 - ((\theta_n - \varphi_n)/\theta_{max})^2]} \\ &+ \frac{\delta}{2} \sum_{m \neq n} (d - |\vec{r}_n - \vec{r}_m|)^2 \Theta(d - |\vec{r}_n - \vec{r}_m|) \end{aligned} \quad (7)$$

with

$$\begin{aligned} M &= \hat{M}\frac{a^2W^2}{\hbar^2\Delta} \qquad \sigma = \hat{\sigma}\frac{a^2\Delta}{W^2} \qquad \delta = \hat{\delta}\frac{a^2\Delta}{W^2} \\ k &= \hat{k}\frac{\Delta}{W^2} \qquad a = \frac{\hat{a}}{a} = 1 \qquad d = \frac{\hat{d}}{a}. \end{aligned} \quad (8)$$

Writing $\vec{r}_n = (x_{1,n}, x_{2,n}, x_{3,n},)$ we can derive the equation of motion for $x_{i,n}$ from the Hamiltonian Eq.(6). The resulting Langevin equations describing the coupled dynamics of the chain and of the polaron is given by

$$\begin{aligned} M\frac{d^2x_{i,n}}{dt^2} + \Gamma\frac{dx_{i,n}}{dt} + F(t) + \sum_m \frac{dU_m}{dx_{i,n}} \\ - g\sum_k \sum_{m<k} \frac{dJ_{km}}{dx_{i,n}}(\phi_k^*\phi_m + \phi_m^*\phi_k) &= 0 \\ i\frac{d\phi_n}{dt} - 2\phi_n + \sum_{m \neq n} J_{nm}\phi_m + g|\phi_n|^2\phi_n &= 0, \end{aligned} \quad (9)$$

Thermal fluctuations are incorporated by adding a delta correlated white noise $F(t)$ which satisfies

$$< F(0)F(s) >= 2\Gamma k_B T\delta(s). \tag{10}$$

Note that we also have

$$\overline{k_B T} = k_B T\frac{W^2}{\Delta} = k_B T W g \tag{11}$$

and, as the equation for x_i is expressed in units of $W^2/(\Delta a)$, we have $\Gamma = \hat{\Gamma}a^2/\hbar$. Note that the electron field ϕ_n is coupled to the phonon field $x_{i,n}$ through the function J_{nm}.

Physical Parameter Values. – In order to study the feasibility of the mechanism of the energy transport via polarons for biologically relevant systems we have used the parameter values corresponding to Amid-I vibrations in α-helices [15]: $W \approx 2\times 10^{-22}J \approx 1.2meV$, $\hat{\sigma} = 19.5N/m$ and $\hat{M} = 2\times 10^{-25}kg$. $a \approx 0.45nm$. $\epsilon = 0.02eV$. $\Delta = 8\frac{\epsilon^2}{\hat{\sigma}} = 4.74\times 10^{-22}J = 0.003eV$. Moreover, $\hat{k}$ can be evaluated from the persistence length of α-helices $\lambda \approx 65nm$ [16]

$$\hat{k} = \lambda k_B T/a \approx 6\times 10^{-19}J. \tag{12}$$

Though we do not have experimental values of $\hat{\delta}$, it is clear that it must be larger than $\hat{\sigma}$. For the friction coefficient we assume that $\hat{\Gamma} \approx 6\pi\mu a$, where $\mu = 0.001Pa\,s$ is the water viscosity. Incidentally, for the cytoplasm μ is up to 4 times larger than this value.

At "room" temperature $T = 300K$, the non-dimensional parameter values are

$g = 2.5$	$\sigma = 51351.$	$k = 7776$	$\Gamma = 8143$
$M = 2.79\times 10^5$	$k_B T = 54$	$\nu = 0.01$	$\tau_0 = 10^{-12}s.$

Following Mingaleev *et al.* [14] we choose $\alpha = 2$. For these parameters, the polaron turns out to be spread over a few lattice sites.

Next we performed simulations of Eq.(9) to explore the coupled dynamics of polaron transport and the conformational transitions of the chain associated with such motion. For the values of g and k mentioned above, we found that the physical α-helices are too rigid for the polaron to bend the chain and move along it as suggested for DNA in [14] (see Fig. 2 in [14] where our g corresponds to N).

As a matter of fact, physical polarons always have a relatively small energy, too small to bend a polymer spontaneously, even for DNA. Nevertheless, the Mingaleev et al. model can be used to study the properties of polarons on chains that are, like most proteins, naturally bent. As a kink in the chain reduces the distance between nodes that are not adjacent to each other, and hence the energy of the configuration, one expects that the polaron would be attracted by the kink. Thus chain conformations where the angle between consecutive tangent vectors increases monotonically could serve as attractive potentials for the polaron, which would accelerate towards regions of high curvature. Nevertheless, the fact that the polaron can move is not as trivial as it may seem at first sight. First, the polaron is spread over several lattice sites and, as the phonon field is coupled to the electron, it is not obvious, a priori, how the energy minimum will be achieved. Moreover, due to the discrete nature of the lattice the polaron is trapped by the so called Peierls-Nabarro barrier which must be overcome by the polaron before it can start moving.

In the next section we present the results of investigations of whether these expectations are correct for proteins.

Polaron on a Bent Chain. – We consider a chain of $N = 60$ points with a bent mid-section *i.e.* the region between $n = 25$ and $n = 45$. Such a configuration is achieved by setting, initially, φ_n as follows:

$$\begin{array}{ll} n < 25 & \varphi_n = 0 \\ 25 \le n \le 45 & \varphi_n = (n-25)d\varphi \\ n > 45 & \varphi_n = 0, \end{array} \tag{13}$$

where $d\varphi$ is the incremental increase in the angle between adjacent links. Our choice of using 60 lattice points was made to ensure that the edge effects were negligible and to have a bent section that was long enough. Had the bent region had a slightly different length, the polaron oscillations in Fig 1 would have changed accordingly, but the overall results would not have been affected.

In order to numerically simulate the dynamics of the polaron on such a chain, we initially generated and saved the polaron on an undeformed (*i.e.* straight) lattice ($\varphi_n = 0$ for all n). Such a polaron was obtained by a relaxation method: a friction term was added to the phonon field and the eigenvalue problem for the electron field was solved simultaneously by relaxation. Starting with an electron spread over a few lattice sites and located on a node which we have chosen to be $n = 30$, the system was relaxed until both the electron and the phonon fields reached a stationary configuration. This produced a polaron configuration centred at $n = 30$. The lattice was then deformed by changing the values of φ_n to those of (13) and a second relaxation was performed to let the phonon field reach its equilibrium configuration. The electron field of the relaxed polaron was then restored, the time set to $t = 0$, and the equations for the phonon and electron fields integrated numerically.

The zero temperature ($T = 0$) dynamics was obtained by numerically integrating the electron and phonon fields in Eq.(9) employing a fourth order Runge-Kutta scheme, noting the time it took for the electron to start moving.

Fig. 1 summarises our results for $T = 0$. Panel (a) shows typical trajectories of a polaron for different values of α, the parameter that models the range of the long-ranged interaction J_{mn} (Eq.(2)) Our simulations show that the main effect of including the next to the nearest neighbour interaction is to make the polaron "to get

attracted" to the bend as lattice points near this bend are nearer to each other, lowering the energy of the polaron. Hence, on a bent chain, with a slowly increasing bending angle, the polaron is attracted increasingly to the bend as it moves along the chain. This corresponds to the spontaneous displacement of the polaron. It is curious to note that upon reaching the edge of the bent chain beyond which the chain is straight the polaron is reflected. This can be explained by the fact that the energy of the polaron is the lowest where the bending angle is large and the highest where the chain is straight. The transition from a bent to a straight configuration thus corresponds to a potential wall on which the polaron bounces. One notices also that as the parameter α is increased the exchange energy between non adjacent nodes decreases more rapidly with the distance separating them. This results in a smaller acceleration of the polaron as seen in Fig. 1. The speed of the polaron was evaluated as $V = [n(t_0 + \Delta t) - n(t_0)]/\Delta t$ where t_0 is the time at which the polaron started to move and $\Delta t = 50$. When the polaron travelled a distance larger than 20, we took $V = 20/\Delta t$ where Δt was the time taken to cover this distance.

Fig. 1(b) shows the chain configuration with the electron density superimposed on it. Each filled circle (black) corresponds to a lattice point, while the electron density, denoted in grey/yellow, is overlayed on them. The intensity of the lighter circles provides a measure of the electron density at a particular site, *i.e.* a lighter colour corresponds to a higher electron density. The maximum in the electron density corresponds to the position of the polaron used to generate Fig. 1(a).

Next we have investigated the dependence of the polaron dynamics on $d\varphi$ - the gradient of the bending angle of the chain. Fig. 2 shows the variation of the average velocity $\langle V \rangle$ as a function of $d\varphi$. For our choice of parameter values the polaron does not move until a critical value $d\varphi \approx 0.0056$ is reached. The dependence of the velocity on $d\varphi$ in the critical region follows a power law $\langle V \rangle \sim (d\varphi - d\varphi_c)^\nu$ akin to elastic depinning of interfaces. In order to express the average speed in physical units, we have to multiply the dimensionless speed by $a/t \approx 328.5 \frac{nm}{ns}$. Thus the average speed of the polaron $\langle V \rangle \approx 16 nm/ns$.

In order to study the effect of thermal fluctuations on the polaron transport we have performed finite temperature $T \neq 0$ simulations. For such simulations we generated a polaron on a straight lattice at $T = 0$ as above and saved it. Next, we deformed the lattice into a bent configuration as above and integrated our equations for 300 units of time to ensure thermal equilibrium. We then restored the electron field, without altering the phonon field, and numerically integrated Eq (9) with the noise term to investigate the motion of the polaron along the chain. This simulation strategy, faithfully mimics the sudden excitation of a polaron and its time evolution.

When one introduces a non-zero temperature, the polaron shape starts to wobble. If the temperature is large

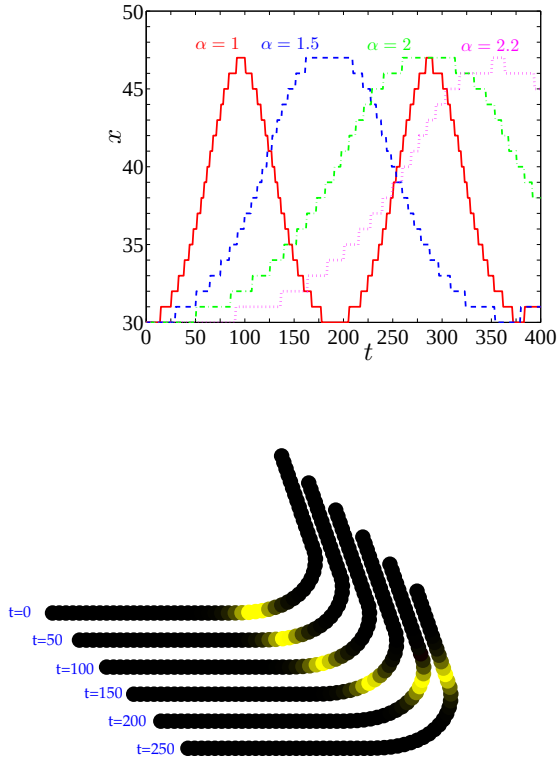

Fig. 1: Polaron displacement on a bent chain with $d\varphi = 0.01$ at $T = 0$ for a $N = 60$ chain with the initial polaron position at $x_0 = 30$. The time step of integration is chosen to be $dt = 50$. Panel (a) shows the trajectory of the polaron on the bent chain for different values of α ($\alpha = 1$ (red solid line), $\alpha = 1.5$ (blue dashed line), $\alpha = 2$ (green dash-dotted line), and $\alpha = 2.2$ (magenta dotted line). Panel (b) shows the chain configuration and the electron density. Each circle corresponds to a node and a lighter colour corresponds to a higher electron density.

enough to overcome the trapping by the Peierls-Nabarro potential ($T > T_c \approx 0.003K$), the polaron starts a random walk which increases in amplitude with the temperature. Our finite temperature studies have focused on the polaron dynamics at "room temperature", *i.e.* $T = 300K$. Clearly, the effects of taking non-zero temperature are very significant as seen in Fig. 3. It is clear from this figure that the polaron undergoes large amplitude fluctuations about its initial position and its velocity is significantly altered by the thermal effects. The thermally averaged polaron velocity shown in Fig. 3 is averaged over $N_{run} = 1000$ simulations, each time having measured the average displacement over $t = 50$ units of time. In all cases the life time of the polaron was of the order $t = 200$, in our units, which corresponds to about $300ps$. Afterwards the electron was delocalised on the lattice. In Fig. 4 we have plotted the variation of the thermally averaged velocity as

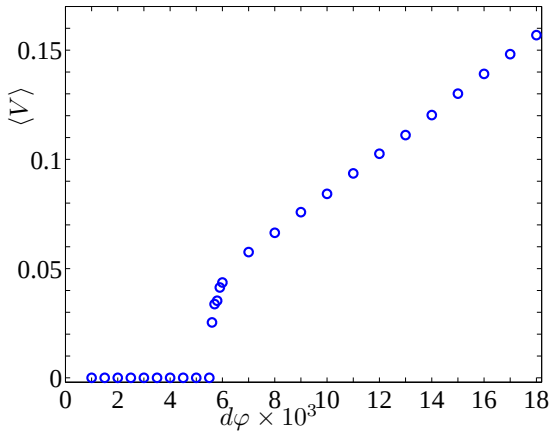

Fig. 2: Figure showing the variation of the velocity $\langle V \rangle$ as a function of the bend angle $d\varphi$ for a bent chain of $N = 60$ nodes. The initial position of the polaron is at $x_0 = 30$, the bent region extends from $n = 25$ to $n = 45$ and $T = 0$. The speed was computed as $V = d/\Delta t$ where $\Delta t = 50$ and d is the distance travelled by the polaron during this time interval.

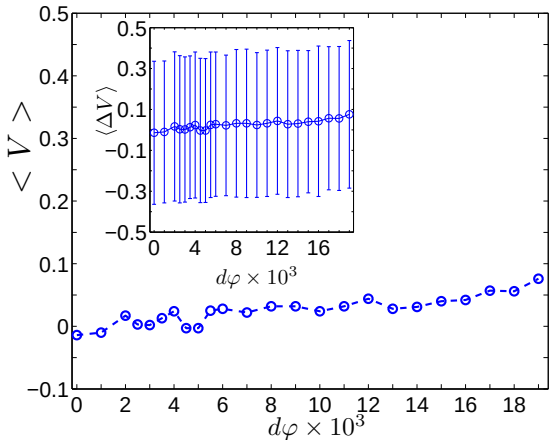

Fig. 3: Figure shows the variation of the average velocity $\langle V \rangle$ as a function of the bend angle $d\varphi$ for a $N = 60$ chain. The chain is bent between $n = [25, 45]$ nodes, and the initial position of the polaron is at $x_0 = 30$. The temperature $T = 300K$, and the data is averaged over $N_{run} = 1000$ simulations. The speed was evaluated exactly like in figure 2. Inset shows the variance of the velocity vs. $d\varphi$ data.

a function of $d\varphi$; this is to be compared with the curve obtained for $T = 0$ in Fig. 2.

Our simulations clearly show that the thermal effects lead to a wider displacement of the polaron which can involve motion in both directions. The polaron is thus subjected to a random walk motion in a system with an attractive force provided by the bend of the chain. So, while the displacement of a polaron in a protein at room temperature is random, its position is still biased by the bending gradient; a thermalised polaron thus follows a random walk, but its average displacement is similar to that of a polaron at $T = 0$.

In order to quantify the dependence of the bend on the spontaneous transport of polarons we have calculated the dependence of the critical incremental angle between segments $d\varphi_c$ on its initial distance from the bend at $T = 0$. This is shown in Fig. 4. It is clear from the plot that $d\varphi_c \propto \exp[-\xi L]$, where ξ is a constant and L is the distance between the polaron and the edge of the region with the bend.

Finally we have also explored a possible mechanism of the energy/polaron transport for biomolecules *i.e.* α helices in our case. Thus we have considered the transport of polarons on straight chains at finite temperatures. Since the edges of the chains act as reflecting walls a polaron that is initially formed close to one edge of the chain will get reflected from it during the course of its random walk motion with an amplitude set by the thermal energy scale. Fig. 5 shows the dependence of the mean position of such a polaron that has initially been created at $x_0 = 5, 10, \ldots 25$. While the steady state polaron position is the same for all values of x_0, their early time behaviour is significantly different. Thus a polaron formed at $x_0 = 5$ has a high average velocity due to its reflections from the $n = 0$ edge and is, on average, transported further at a given time (say $t = 140$) than a polaron formed at $x_0 = 25$. This compels us to conjecture the following model of polaronic transport for biophysical systems: if a polaron is generated by electron-phonon interactions near an edge of a short straight segment of a protein it will undergo reflections from the nearby edge, leading to the directed motion towards the other edge. When the system contains receptor molecules that can absorb this non-linear excitation and transfer it to other molecules or polymers, the polaron displacement can be used to transport the energy released by ATP hydrolysis to a nearby regions of the cell where it is needed.

Conclusions. – In this paper we have studied the transport of energy along bio-polymers via polaronic mode. Starting from a model that describes coupled electron phonon dynamics, we chose physically relevant parameter values and studied polaron dynamics on bent configurations of bio-polymers. We have found that the bent chain induces spontaneous polaron transport due to some of its nodes being closer together and so generating an attractive potential for the polaron. At $T = 0$, polaron movements were observed in proteins for small gradient of the bend ($d\varphi < 0.0055$ in our units). The polaron moved at a speed $V \approx 16nm/ns$ and lived for about $t = 300ps$. At $T = 300K$, the polaron exhibited a random walk motion biased in the direction of the bending gradient. The bending gradient of the chain thus induced an average polaron displacement. Moreover, on a straight chain, we observed that a polaron near the edge of the chain exhibits spontaneous displacement in the direction away from the edge. We have thus shown that polaron displacement can be induced spontaneously without the need to kick the polaron in one direction and that the direction of transport can be determined by the configuration of the polymer.

Polaron states have been experimentally observed in

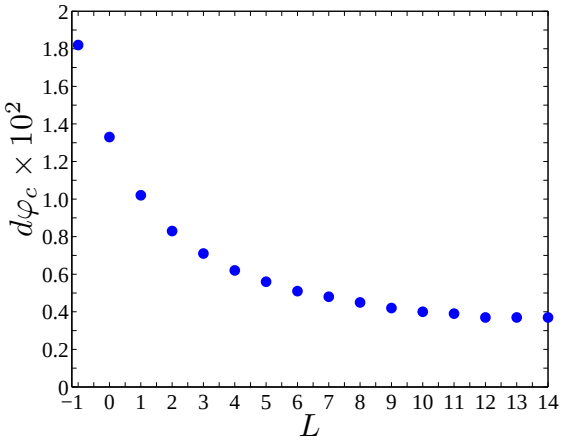

Fig. 4: Figure shows the variation of the critical bend angle $d\varphi_c$ as a function of the initial relative polaron position L with respect to the bent region, $n_{0,pol} = 25 + L$. N = 60 and T = 0. The speed was evaluated exactly like in figure 2.

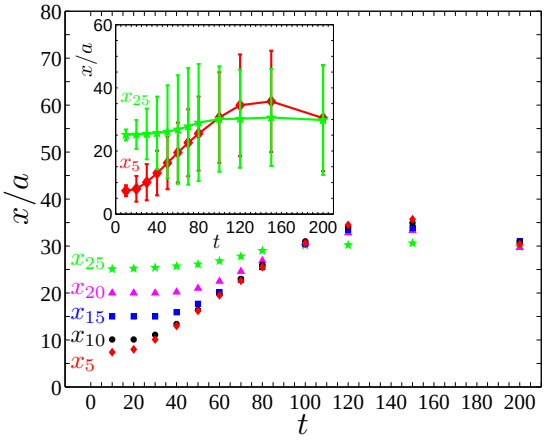

Fig. 5: Figure shows the average position of a polaron as a function of time for a straight chain of $N = 60$ segments at $T = 300K$ for different initial positions ($x_i = 5$ (red diamonds), $x_i = 10$ (black circles), $x_i = 15$ (blue squares), $x_i = 20$ (magenta upper triangles) and $x_i = 25$ (green stars)) averaged over $N_{run} = 1000$. Inset shows the average position and the fluctuation about the mean position of the polaron for two initial positions $x_i = 5$ and $x_i = 25$.

several proteins including the B850 aggregate of the Light Harvesting 2 trans-membrane complexes [17–19]. LH 2 is particularly relevant to our work as its contains the alpha-helix B850, spanning the width of the cell membrane, and it exhibits a steady gradient bend [20] similar to the one we have used in our model. Our study thus predicts that the polaron in the B850 will move spontaneously because of the shape of the B850.

Finally, we would like to mention that in our model we have not taken into account the effects that water molecules could have on the polaron size as this would require a quantum-mechanical treatment of the polaron system. In fact the effect of water on the DNA polarons may lead to the reduction of their size and to their confinement onto a single lattice site [21, 22]. As DNA and alpha-helix polarons have very different properties (the dimensionless non-linear coefficient g is about twice as large for alpha-helices than for DNA and alpha-helices are more rigid than DNA) it is not clear whether water would have a similar effect on protein polarons.

* * *

Acknowledgement. – BC was partially supported by EPSRC grant EP/I013377/1. BP and WJZ were supported by the STFC research grant ST/H003649/1.

REFERENCES

[1] Davydov A. S., *J. Theor. Biol.*, **38** (1973) 559;Davydov A. S.,*Phys. Scr.*, **20** (1979) 387;Davydov A. S.,*Phys. D*, **3** (1981) 1.
[2] Davydov A. S., *Solitons in Molecular Systems*, edited by D. Reidel (Dordrecht) 1985; Davydov A. S.,*J. Theor. Biol.*, **38** (1973) 559.
[3] Scott A. C., *Phys. Rep.*, **217** (1992) 1.
[4] Cruzeiro L., *J. Biol. Phys.*, **35** (2009) 43.
[5] Olsen O. H. *et al.*,*Phys. Rev. A*, **38** (1988) 5856; Olsen O. H., Lomdahl P. S. and Kerr W. C.,*Phys. Lett. A*, **136** (1969) 402.
[6] La Magna A., Pucci R., Piccitto G., and Siringo F.,*Phys. Rev. B*, **52** (1995) 273
[7] Zolotaryuk V., Christiansen P. L., and Savin A. V, *Phys. Rev. E*, **54** (1996) 3881.
[8] Christiansen P. L., Zolotaryuk V., and Savin A. V., *Phys. Rev. E*, **56** (1997) 877.
[9] Henning D.,*Phys. Rev. B*, **65** (2002) 147302.
[10] Kalosakas G., Aubry S., and Tsironis G. P., *Phys. Rev. B*, **58** (1998) 3094.
[11] Voulgarakis N. K and Tsironis G. P., *Phys. Rev. B*, **63** (2001) 014302.
[12] Brizhik L., Eremko A., Piette B. and Zakrzewski W. J., *Phys. Rev. E*, **70** (2004) 031914.
[13] Brizhik L., Eremko A., Piette B. and Zakrzewski W. J., *J. Phys. : Condens. Matter.*, **22** (2010) 155105
[14] Mingaleev S. F., Gaididei Y. B., Christiansen P. L. and Kivshar Y. S., *Europhys. Lett.*, **59** (2002) 403.
[15] Scott A. C., *Phys. Rev. A*, **26** (1988) 578.
[16] Phillips G. N., Chacko S., *Biopolymers*, **38** (1996) 89
[17] Wu H.-M., Ratsep M., Jankowiak R., Cogdell R.J., and Small G.J., *J. Phys. Chem.*, **B 101** (1997) 7641
[18] Reddy N.R.S., Picorel R. and Small G.J., *J. Phys. Chem.*, **96** (1992) 6458
[19] Freiberg A., Rätsep M., Timpmann K. and Trinkunas G., *Journal of Luminescence*, **102-103** (2003) 363
[20] Koepke J., Hu X., Muenke C., Schulten K. and Michel H., *Current Biology*, **4** (1996) 581
[21] Kravec S.M., Kinz-Thompson C.D. and Conwell E.M. , *J. Phys. Chem.*, **B 115** (2011) 6166
[22] Thazhathveetil A.K, Trifonov A., Wasielewski M.R. and Lewis F.D., *J. Am. Chem. Soc.*, **133** (2011) 11485